Journal of Hazardous Materials 177 (2010) 602–612

Contents lists available at ScienceDirect

Journal of Hazardous Materials

journal homepage: www.elsevier.com/locate/jhazmat

Interaction of debris with a solid obstacle: Numerical analysis

Anna Kosinska*

Bergen University College, Faculty of Engineering, P.O. Box 7030, 5020 Bergen, Norway

ARTICLE INFO

Article history:
Received 23 July 2009
Received in revised form
14 December 2009
Accepted 17 December 2009
Available online 23 December 2009

Keywords:
Explosion
Safety
Mathematical modelling
Fluid–structure interaction
Debris–structure interaction
Two-phase flow

ABSTRACT

The subject of this research is the propagation of a cloud of solid particles formed from an explosion-damaged construction. The main objective is the interaction of the cloud (debris) with a solid beam located at some distance from the explosion. The mathematical model involves the flow of the gas using standard conservation equations, and this part of the model is solved numerically. The solid particles are treated as a system of solid points (so-called Lagrangian approach), whose motion is the result of the flowing gas as well as collisions with obstacles. These two issues are described respectively by Newton's second law and the hard-sphere model. The model is used to simulate various cases where the influence of different parameters like the value of the pressure of the explosion, the particle size, the number of particles and the obstacle location are investigated. The results are presented as snapshots of particle location, and also as the particle total momentum during collision with the beam.

1. Introduction

Modelling of the interaction of a fast-moving flow with a structure requires using proper computational tools that can deal with this multi-physics problem. The flow is usually modelled using computational fluid dynamics (CFD) techniques, while the behaviour of the structure is done by applying codes using the Finite Element Method. This paper focuses on the first problem, and a technique that can simulate the flow of debris resulting from an explosion has been developed. This technique is based on the so-called Eulerian–Lagrangian modelling, normally used to simulate two-phase flows (see e.g. [1]). Our objective is to adapt this approach for our needs.

CFD has been extensively used to study gas/dust explosions and innumerable publications have dealt with this problem. An explosion usually leads to the formation of a strong pressure wave that propagates in the computational domain, and interacts with the obstacles and other solid bodies. This has many applications ranging from pure scientific interest to important practical ones such as explosions.

In the literature several papers dealing with the issue of the response of a solid structure to a sudden flow of gas can be found. However, most of these works consider blast waves from explosives, while a little less focus has been given to what could happen to a construction after a gas/dust explosion. In reality, the problems are very similar, though the "explosion characteristics" are quite different. Studying some selected publications dealing with these problems, indicates a general trend.

The literature overview on explosions reveals Eckhoff's books as the most recent and extensive Refs. [2,3], which describe the entire physics of the problem. However, the issue of explosion/construction interaction is only briefly described. Clutter et al. [4] show some CFD results on an explosion propagation that is simulated in some modelled urban area. The model is based on the compressible Euler equations, and therefore their paper is quite similar to this research paper (see next section). They used a one-step chemical reaction process that had been tested earlier that produced satisfactory results. What they show are pressure histories measured at some monitor points in the computational domain. This illustrates how the complex geometry influences the results, as well as emphasizes the need to use advanced computational techniques to study these interesting problems.

The paper by Lu and Xu [5] is also somewhat related to our research. The authors present a model that is able to predict the initial velocity of debris resulting from an internal explosion in a concrete vessel. They analyse the wall material and create a mathematical model that describes its behaviour. Various cases are analysed and the results are compared with experimental findings. Where their papers differ from this one is that, here we do not model the exact behaviour of the material that is damaged during an explosion, but rather the further consequences.

Many authors use some commercial software (usually AUTODYN) to analyse the exact behaviour of the construction due to a sudden load. For example Luccioni et al. [6] analyse a concrete

* Tel.: +47 555 87742; fax: +47 555 87790.
E-mail address: adk@hib.no.

0304-3894/$ – see front matter © 2009 Elsevier B.V. All rights reserved.
doi:10.1016/j.jhazmat.2009.12.075

building and its collapse due to a TNT explosive. Also Shi et al. [7] analyse the RC columns and their damage in a similar situation. Finally, experimental techniques have been also widely used (e.g. [8]). Other such works include: Sprague and Geers [9] or Ross et al. [10].

Not only is this study focussed on explosions and structures, it also addresses the issues of interaction of a strong pressure wave with a cloud of particles. A short literature overview on this topic follows.

Some of the most recent work has been done by Igra and Jiang [11] who analyse the problem of the first interaction and behaviour of the shock wave. Their tool is a computer code that solves the solid phase using the Eulerian approach (the solid particles are treated as a second fluid). Bedarev et al. [12] use the Lagrangian approach to model shock-wave interaction with particles in a cavity.

Federov et al. [13] analyse two problems, where the first one is the interaction of a shock wave with a layer. The results are compared with experimental observations. Suzuki et al. [14] perform interesting experiments as they study the behaviour of solid particles behind shock waves, where the particles initially form a layer. A case when both the dust phase and some element of geometry are present in the system is thoroughly studied by Igra et al. [15]. Their objective is the analysis of shock-wave interaction with a wedge, where the solid phase forms a surrounding environment.

Some examples of other works are: Igra et al., Thevand and Daniel, Saito, Klemens et al. [16–19].

The objective of this research is to first combine some of the issues mentioned above: the propagation of the shock wave and its interaction with the cloud of solid particles and an obstacle. We investigated an explosion in a closed domain that resulted in a cloud of solid particles (i.e. the damage of the construction). The debris propagates further away due to the intense gas flow and interacts with a solid obstacle.

This paper differs from the above mentioned work in the detailed analysis of the debris interaction with some construction elements, in this instance, with a solid beam that is located at a specified distance from the explosion. First, the mathematical model (see the next section) was carefully selected and then simulations were performed, where the following important parameters could vary: explosion intensity, particle size, particle number and beam location. As the influence of some of the parameters is rather obvious, we also obtain less expected results.

2. Model

Modelling of the consequences of a gas explosion where debris is produced requires the analysis of a few phenomena that occur at the same time. One is the gas flow in a domain with a complex geometry with combustion and interaction with the solid bodies. In some cases, however, there is no necessity to analyse all the details, as in this paper, where the focus is only on the behaviour of the debris. Therefore, it is not necessary to model the chemical reactions: assuming that the origin of the explosion is a domain with high pressure and temperature is quite sufficient. This will lead to strong pressure waves being formed that mimic the explosion.

The second issue is the motion of the debris, which really is a system of solid particles of different shapes and sizes. One approach is to assume that all of them are spherical in shape and of the same diameter. Thus, we may find ready expressions for the aerodynamic force between the gas and the solid particles (the drag force). The motion of the particles can be modelled using the standard Newton's second law.

The first part of the model that corresponds to the above mentioned description is given below.

2.1. Model for the gas phase

We model the gas flow using the well-known Euler equations for compressible flow:

$$\frac{\partial \rho}{\partial t} + \nabla \cdot (\rho \vec{u}_g) = 0 \tag{1a}$$

$$\frac{\partial \rho \vec{u}_g}{\partial t} + \nabla \cdot (\rho \vec{u}_g \otimes \vec{u}_g) = -\overrightarrow{\nabla p} - \sum \vec{f}_i \tag{1b}$$

$$\frac{\partial E}{\partial t} + \nabla \cdot [\vec{u}_g (E + p)] = -\sum \vec{f}_i \cdot \vec{u}_{p,i} - \sum q_i \tag{1c}$$

The first Eq. (1a) is the continuity equation with ρ being the gas density and $\vec{u}_g$ the gas phase velocity. The second Eq. (1b) is the momentum conservation equation where p is the pressure and $\sum \vec{f}_i$ represents the sum of the forces from the solid particles (debris). This is described below. The third Eq. (1c) is the energy conservation equation with E being the total energy of the gas in unit volume, $\vec{u}_{p,i}$ is the velocity of ith particle and q_i is the heat transfer rate (also see the details below).

The system of equations also requires a closure, which is the equation of state. Here, we assume the ideal gas law.

2.2. Model for the solid phase

As mentioned above, the cloud of debris can be treated as a system of spherical particles whose motion can be described using Newton's second law:

$$m_i \frac{d\vec{u}_{p,i}}{dt} = \vec{f}_i + m_i \vec{g} \tag{2}$$

where the subscript i denotes the ith particle and m is particle mass.

Note that Eq. (2) describes the motion of ith particle only. Therefore, the number of these equations must equal the number of particles in the system.

The force $\vec{f}_i$ in the model is the drag force between the gas phase and the particles. This is modelled using the well-known expression (see e.g. [1]):

$$\vec{f}_i = C_D(\mathrm{Re}) \cdot A_p \cdot \frac{\rho(\vec{u}_g - \vec{u}_{p,i})|\vec{u}_g - \vec{u}_{p,i}|}{2} \tag{3}$$

where $C_D(\mathrm{Re})$ is a coefficient dependent on the relative particle Reynolds number Re, and A_p is the projected area. In this research, the following empirical formulae were used (e.g. [20]) that gives the value of the coefficient approaching Newton's law as the Reynolds number increases:

$$C_D = \frac{24}{\mathrm{Re}} \left[1 + 0.183\sqrt{\mathrm{Re}}\right] + 0.42 \tag{4}$$

The relative Reynolds number is defined as: $\mathrm{Re} = \rho \cdot d \cdot \left|\vec{u}_g - \vec{u}_{p,i}\right| / \mu$, with d being particle diameter. The typical value of the Reynolds number in the simulations may vary from zero (as the relative velocity is also zero) until around 20 000 for the values used in the simulations (as the shock wave encounters the particles).

Since the particles may also rotate, this is described using the model below,

$$I_i \frac{d\vec{\omega}_i}{dt} = \vec{M}_i \tag{5}$$

where I_i is the moment of inertia, $\vec{\omega}_i$ is the angular velocity and $\vec{M}_i$ is the torque. The source of the torque is usually the shear from the flow, acting on the particle surface. This effect is actually negligible compared with the much more important effect than the collisions of the particles with the solid walls present in the computational domain. Therefore, we ignore this effect.

The next problem is the heat transfer between the particles and the gas. As no chemical reactions are assumed, this effect is less urgent to model. However, there is a possibility of obtaining some cooling effect of the hot gas, and this will influence its behaviour. Therefore, we consider it in the modelling by assuming the forced convection between the particle surface and the flow:

$$\frac{dT_{p,i}}{dt} = \frac{1}{m_{p,i}c_p} q_i \tag{6}$$

where $T_{p,j}$ is the particle temperature and c_p is its heat capacity.

The heat transfer rate is described by the standard expression:

$$q_i = A \cdot Nu \cdot k/d \left(T_g - T_{pi}\right) \tag{7}$$

where Nu is the Nusselt number, k is conductivity of the gas phase, A is particle surface area and T_g is the temperature of the gas phase.

The Nusselt number was modelled as follows:

$$Nu = 2 + 0.6\sqrt{\mathrm{Re}}\mathrm{Pr}^{1/3} \tag{8}$$

with Pr being the Prandtl number.

2.3. Collisions

As a particle approaches a solid wall or another particle, it may be a subject to a collision. The most interesting for us especially, are the collisions with a structure. This leads to a sudden increase in stress and a possible fracture. In this paper, the behaviour of the solid structures is not modelled, as the problem of the response of the construction has been widely researched earlier.

To study the collisions, the hard-sphere model was used. A precise description for both particle–particle and particle–wall collisions can be found in e.g. [1]. In this paper we focus on the particle–structure interactions, i.e. we study how the behaviour of the particle cloud may lead to stresses in the construction. Therefore we do not present the exact model for particle–particle collisions, bur rather emphasize the particle–wall collisions. Both models are, however, included in the computational code.

In our simulations the collision model is necessary to account for both particle–obstacle collisions, as well as particle collisions with the lower wall. The second effect is especially more visible for particles with a higher inertia as shown later in the paper.

As a particle approaches a wall its initial velocity has the following components: $\vec{u}_{p,i} = (v_x^{(0)}, v_y^{(0)}, v_z^{(0)})$ and $\vec{\omega}_i = (\omega_x^{(0)}, \omega_y^{(0)}, \omega_z^{(0)})$. The coordinate system is thus described: y-axis is normal to the plane of collision, while x- and z-axes are in the plane of the wall.

During the impact two periods can be clearly distinguished: compression and restitution. In both periods there is a normal impulse acting outwards (i.e. along y-axis). Here, we define the coefficient of restitution, e, that expresses the ratio between the normal component of this impulse in the compression period to that in the recovery period. This coefficient may vary between 0 and 1, where 0 corresponds to a fully non-elastic collision, and 1 corresponds to an elastic collision where no energy is lost.

The new velocities after the collision with the wall are (see [1]):

$$\begin{aligned} &v_x = \frac{5}{7}\left(v_x^{(0)} - \frac{2r}{5}\omega_z^{(0)}\right); \quad v_y = -ev_y^{(0)}; \quad v_z = \frac{5}{7}\left(v_z^{(0)} + \frac{2r}{5}\omega_x^{(0)}\right) \\ &\omega_x = \frac{v_z}{r}; \quad \omega_y = \omega_y^{(0)}; \quad \omega_z = -\frac{v_x}{r} \end{aligned} \tag{9}$$

for the case when:

$$\frac{v_y^{(0)}}{|v|} < -\frac{2}{7f(e+1)}$$

and

$$\begin{aligned} &v_x = v_x^{(0)} + \varepsilon_X f(e+1)v_y^{(0)}; \quad v_y = -ev_y^{(0)}; \quad v_z = v_z^{(0)} + \varepsilon_Z f(e+1)v_y^{(0)} \\ &\omega_x = \omega_x^{(0)} - \frac{5}{2r}\varepsilon_Z f(e+1)v_y^{(0)}; \quad \omega_y = \omega_y^{(0)}; \quad \omega_z = \omega_z^{(0)} + \frac{5}{2r}\varepsilon_X f(e+1)v_y^{(0)} \end{aligned} \tag{10}$$

for the case when:

$$\frac{v_y^{(0)}}{|v|} > -\frac{2}{7f(e+1)}$$

where r is particle radius ($r = d/2$).

In the above, other parameters are also used: f is the friction factor between the particles and the wall and ε_X and ε_Z are the two factors indicating the proportion of the velocity in each component direction (for a 2D collision in the x–y plane they are equal to 1.0 and 0.0, respectively).

3. Numerical scheme

The mathematical model presented above consists of issues that need to be considered while solving numerically: the flow of the compressible gas (partial differential equations), the motion of the particles (ordinary differential equations), the coupling between the gas and the particles (ordinary differential equations), and the collisions with the walls and between the particles (analytical equations).

The computational domain is two-dimensional and discretized into square cells where gas parameters (density, velocity, temperature and pressure) are stored. The gas equations (Eq. (1)) are solved using the Godunov scheme (see e.g. [21]). For each time step, the particle equations (see Section 2.2) are simultaneously solved using the Runge-Kutta numerical scheme. The particle behaviour is solved in a loop (for each particle) and as the algorithm detects a collision with e.g. a solid obstacle, the hard-sphere model (see Section 2.3) is used to modify the particle velocity.

The boundary conditions were as follows: no-slip boundary conditions on the surfaces of the solid obstacles, while on all the other boundaries we require that the gradient of all parameters is equal to zero.

The numerical scheme used in this paper is based on algorithms shown elsewhere [22,23] and is not the focus of this study. Therefore, the details are not described here.

4. Parameters

The manner in which the cloud of solid particles interacts with a solid obstacle depends on many factors: the explosion pressure, the size of the exploding domain, the concentration of the debris and particle size, as well as the distance to the obstacle as well as the presence of other objects that may change the flow direction of the exploding gas.

However, it may be difficult to estimate the influence of all these factors. Therefore, in this paper the focus is on the geometry that is presented in Fig. 1. The domain where the gas explodes is assumed to be rectangular and its size is the same for all the cases investigated. From the right-hand side it is “blocked” by a cloud of particles, all of the same size (spherical) and density. It is possible to also analyse other configurations, but this will be done during further research. At some distance to the right, a vertical beam of specific size was identified that we did not change during the simulations for the same reason.

The particles are not connected by any interaction, as it would normally be in reality. On the contrary, our research corresponds to the “worst-case” scenario, i.e. these interactions would actually dampen the strength of the explosion. Therefore, they are safely ignored and the desired issues alone are focussed on.

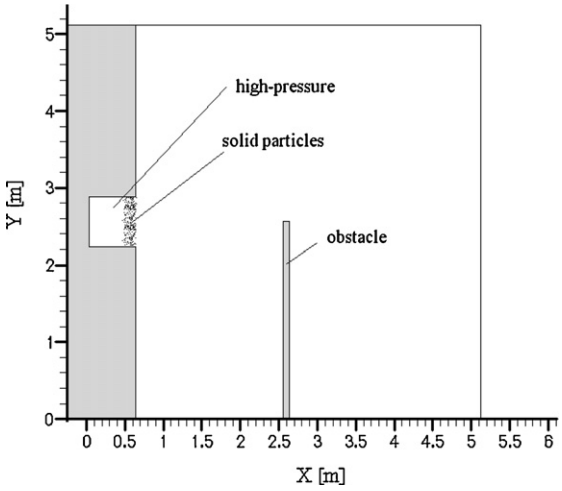

Fig. 1. The sketch of the computational domain.

Another possibility would be to add some "attractive force" that acts between the particles. The value of the force would be a function of the separation between the particles. In order to better quantify the reality this interaction should be strong as the particles are close to each other and then decrease significantly as the distance becomes higher.

As a result the speed of the evacuated gas will be more reduced in comparison to the results presented in this paper. Also higher gas pressure would be recorded in the debris cloud.

The following parameters were not constant: pressure in the high-pressure domain, particle diameter and the distance between the domain and the obstacle. Analysis of only these three parameters produced very interesting results revealing some complex phenomena. Before discussing the results, however, it was worth seeing how the parameters may influence the results, i.e. interaction of debris with the obstacle.

The higher the pressure in the domain, the higher is the initial speed of the particles, and therefore, the faster they would propagate and collide with the obstacle with a higher momentum. In reality it is far more complex: the higher pressure also means that the amount of gas in the domain is higher. The gas, as evacuated, will proceed together with the solid particles and influence their motion. Therefore, it is not enough to mention the "initial velocity of debris", as it is still subject to further interaction with the gas particles as they move.

In practice, the moving gas will also exert some force on the obstacle. This is included in the model presented in this paper, though not emphasized, as this has been dealt with in other works.

Particle size is another interesting parameter. The bigger particles also have a higher inertia, i.e. it takes more time to catch up with the flow, as well as they are later on less influenced by the flowing gas. As the gas interacts with e.g. obstacles, it will change direction and velocity. Heavier particles will be less influenced than the lighter ones.

The location of the obstacle is also significant. If the obstacle is situated very close to the exploding domain, it will be more greatly influenced by the flowing debris. Actually, this is not always the case: if the obstacle is closer to the explosion source, it will also influence the direction of the flowing gas. However, it must be emphasized that the debris is projected with some delay, and as the particles approach the obstacle, they are either slowed down or turned by the gas that has interacted with the obstacle. Thus, the results may be unexpectedly different.

The following parameters were used in this study: the domain was 2D and it was divided into 512×512 computational cells. The physical length and height were 5.12 m. The right and the upper walls were simulated as "open"; thus no physical boundaries were present and the expanding blast waves could freely develop in these directions.

Particle diameter was 2, 4, 6 mm for different cases. Their density was always 1000 kg/m^3 (this parameter is less important as variation of the particle diameter should be sufficient to analyse the issues addressed in this paper) and their initial temperature was 293 K.

The pressure in the high-pressure section varied for different simulations: 4×10^5, 6×10^5 and 8×10^5 Pa. The temperature in this domain was always constant and equal to 1000 K. The size of the high-pressure section was 64×64 computational cells. The obstacle was located in positions 128, 192 and 256 computational cell (for various simulations). The thickness of the obstacle was 8 cells, while the height was 256 cells.

The total number of particles was 2560 (except for one simulation, as mentioned in Section 5.4). The particles were distributed at the right side of the high-pressure section mimicking a wall that has been damaged to an explosion. The thickness of the "wall" was around 14 computational cells.

The force of gravity was also included, with the standard acceleration of 9.81 m/s^2. The ambient pressure and temperature were 1.013×10^5 Pa and 293 K, respectively.

We must emphasize that the objective was not to simulate a real case, like comparing with experimental results or solving a genuine engineering problem. The aim of this study is the analysis of the physical processes that are more of a scientific nature, i.e. to investigate the influence of these parameters and to reveal some complex phenomena.

5. Results

The computer program was validated, right at the beginning. The first part was to compare the results with the analytical solutions. For example, the shock tube problem, whose solution is based on the Riemann problem, or the propagation of a spherical particle whose motion can also be integrated and solved analytically. This usually involves simple one-dimensional cases, but give indication about the robustness and correctness of a computational code.

The second part was to compare with fundamental experimental observations. Here the validation was based on the paper by Boiko et al. [24]. In this reference, the interaction of a shock wave with a cloud of particles was studied. Both particle cloud behaviour as well as gas pressure distribution was given. This made it possible to assess the validity of the code used in this paper.

The third part was to analyse the grid independence where the same case was solved using various grids. The influence of the grid cell size on results like gas pressure or velocity distribution was studied. Also results like the particle location as well as their behaviour (e.g. number of collisions) was controlled using different meshes. It has to be emphasized that using of too fine grids does not lead to physically correct results: the cell size has to be considerably bigger than particle size. Otherwise the primary assumption that the particles are treated as points is not valid any more.

The issue of the interaction of the particles with the solid obstacle involves algebraic formulae, so it does not require validation. These results are not presented in this paper; the focus is only on the problem that we desire to study.

The results in this section are presented showing snapshots of particle position or gas parameters (velocity field, pressure, etc.) for different points in time. Further, the statistical results presented help in understanding these processes, as well as predicting outcomes for other cases that are not dealt with in this research.

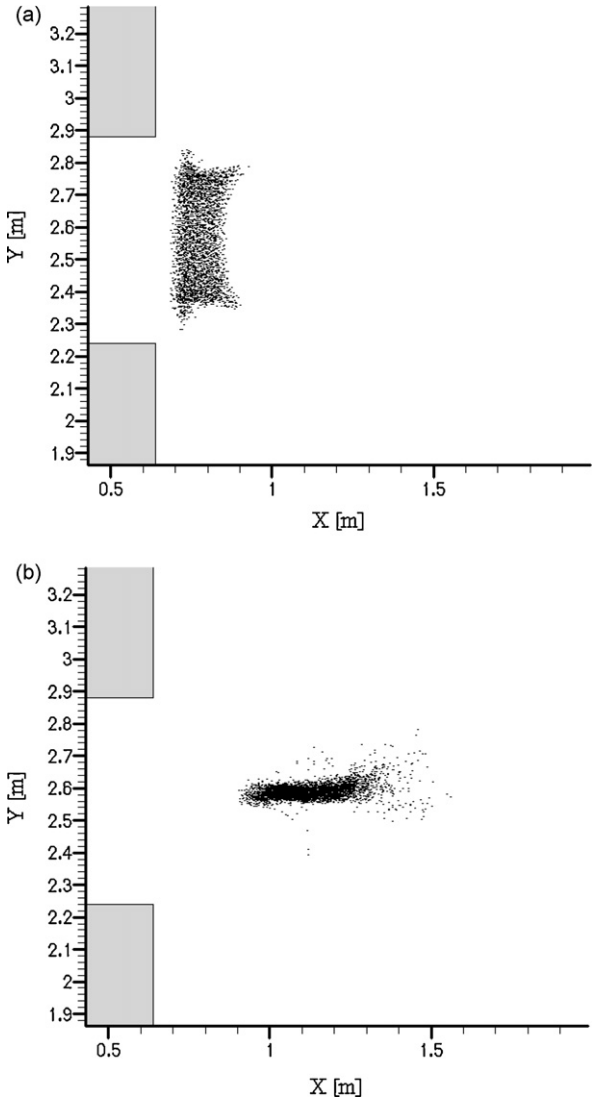

Fig. 2. Two snapshots of particle position after 20 and 60 ms.

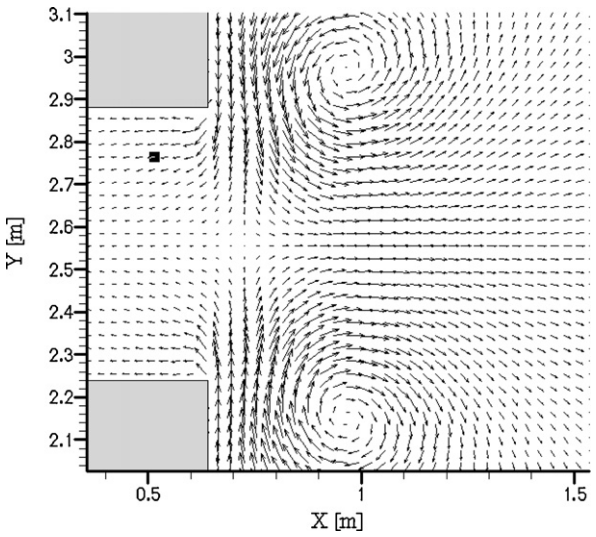

Fig. 3. The gas field velocity close to the chamber exit after 6 ms.

5.1. The process

In this subsection, the process is illustrated by showing some snapshots of particle position as well as gas pressure distributions and velocity fields. The objective is to present the fundamental phenomena necessary to understand more complex issues and facilitate the reader to move to the next sections.

First, two snapshots of particle positions after 20 and 60 ms, i.e. relatively early as we consider the whole processes, are presented (see Fig. 2). The simulation corresponds to the following parameters: particle diameter was 2 mm, the initial pressure in the chamber was 8×10^5 Pa and the obstacle position was 256 grid cells.

The first interesting observation is that the particles are "compressed" towards the central line. This is due to the gas flow that has been evacuated from the high-pressure section as illustrated in Fig. 3. After a few milliseconds, two eddies are observed at the corners, and at the same time, gas flow back to the chamber. This phenomenon is well known in gas dynamics, and in this case, may influence the results in a way difficult to predict. This leads to changing of the particle cloud shape as well as deceleration.

To eliminate this phenomenon, we "removed" the wall on the left side of the high-pressure section, thus forming a huge domain with high pressure, as this type of boundary condition mimicked it. This greatly influences the initial shape of the cloud as well as flow pattern. The results are shown in Figs. 4 and 5 as a snapshot of particle position and the gas velocity field, respectively. When the results are compared with Figs. 2 and 3, a significant difference is evident.

For further simulations, however, the initial geometry was still used, i.e. the size of the high-pressure section was finite, as it was actually more real, especially in rather small-scale explosions.

The next stages of the process are shown in Fig. 6, as subsequent snapshots of particle position showing the interaction of debris with the obstacle. As observed, some particles collide with the beam and bounce off. This also leads to strain in the structure and possible damage. This issue is discussed in subsequent sections.

As mentioned in the earlier section, the beam is also loaded by the exploding gas. The pressure waves actually arrive at the obstacle, before the debris. This problem (the shock-wave phenomena and dynamic loading of structures) has already been extensively studied by many researchers, and is therefore, not repeated in this paper.

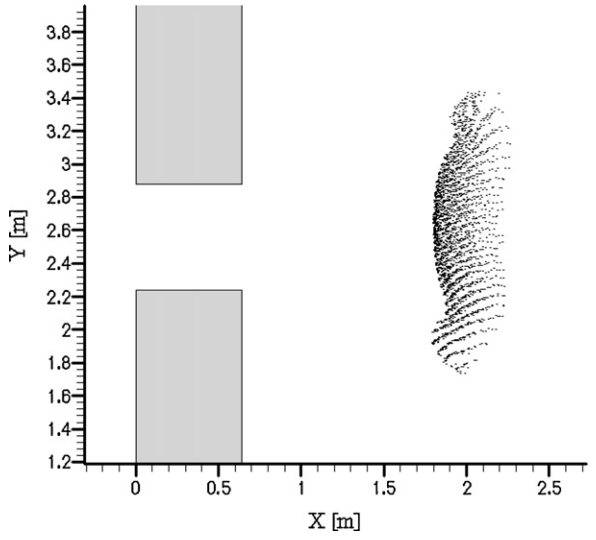

Fig. 4. A snapshot of particle position after 20 ms for the case where the left wall was simulated as "open".

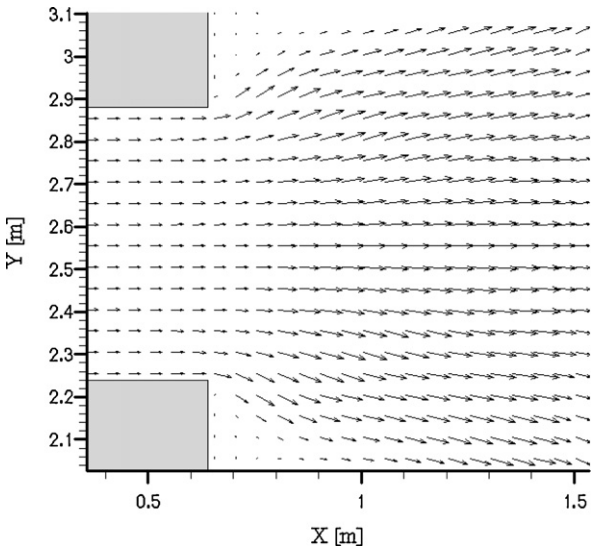

Fig. 5. The gas field velocity close to the chamber exit after 6 ms for the case where the left wall was simulated as "open".

5.2. The influence of the initial pressure

Many parameters may influence the interaction of the debris and the structure. One of the first parameters usually studied is the explosion strength that in this paper is mimicked by the value of the initial pressure in the chamber.

To better evaluate the interaction of the debris with the solid obstacle, a parameter that describes the "strength" of the impact needs to be found. An example is the measurement of the particles' momentum as they collide with the beam.

In this research, simulating the process for the same time period for all the cases was suggested. Then the beam was divided into a number of bands, and later all the particles that collided with each band during this period were analysed. A time period corresponding to 800 ms with the number of bands equal to 10 were selected. Thus, both the "strength of impact" as well as "distribution" over the beam could be investigated. These values here are merely arbitrary and were selected after some testing, to better illustrate the results.

Fig. 7 shows a comparison among three cases, where the initial pressure was 4×10^5, 6×10^5 or 8×10^5 Pa. The curves reveal the total momentum of the particles that collide with the correspond-

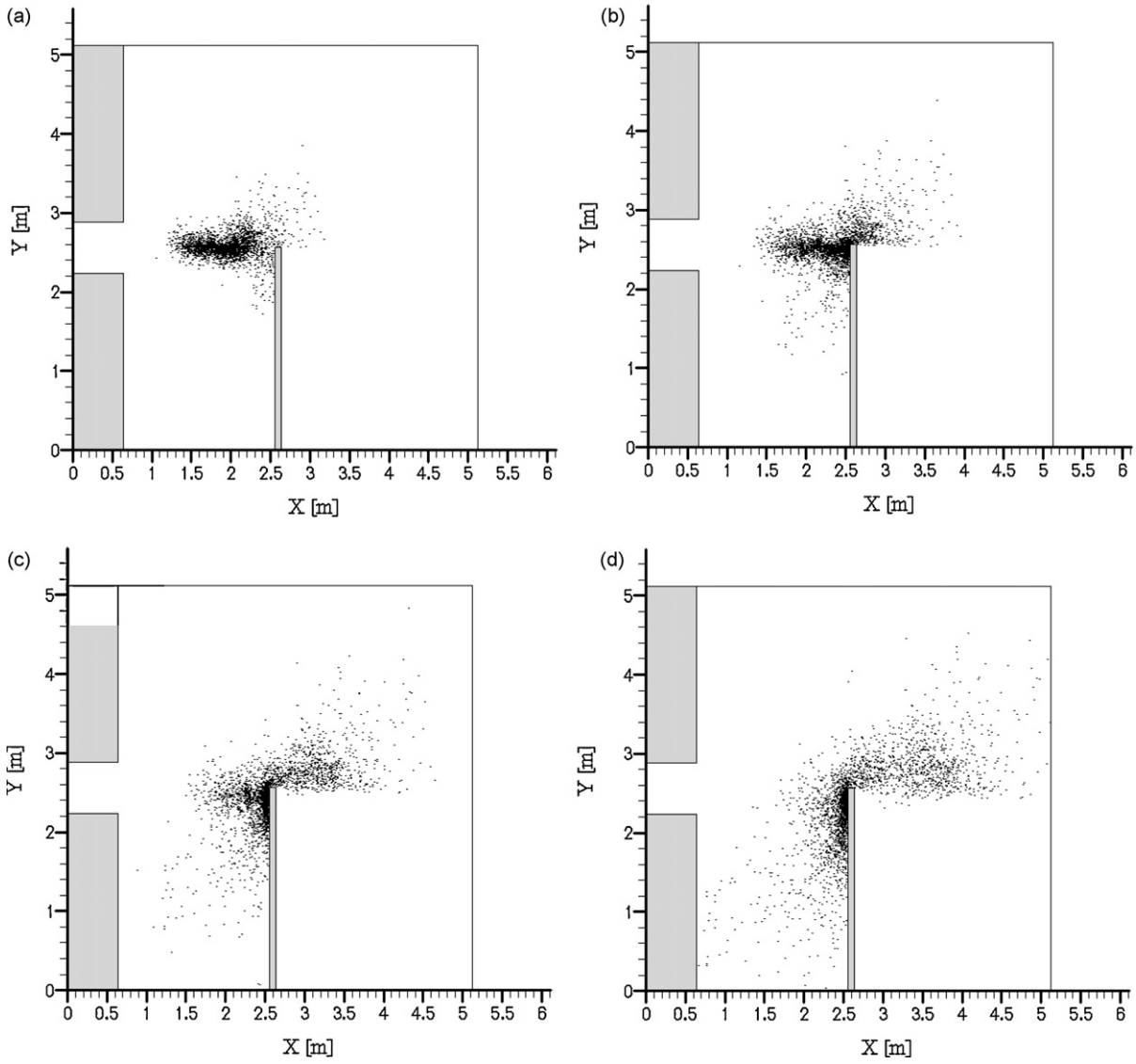

Fig. 6. Snapshots of particle positions for various points in time: (a) 150 ms, (b) 200 ms, (c) 250 ms, and (d) 300 ms. The initial pressure in the high-pressure section was 8×10^5 Pa and particle diameter was 2 mm.

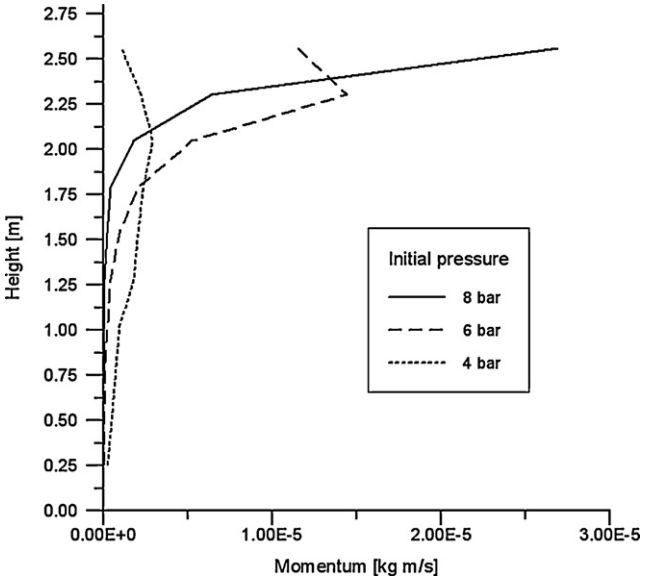

Fig. 7. The distribution of the momentum of particles that have collided with the obstacle for various values of the initial pressure.

ing band. The first conclusion is that the higher pressure led to a higher value of the maximum momentum (this conclusion is rather obvious), but also that the collisions were more "focussed" on the upper part of the obstacle. It is observed that Fig. 6 corresponds to the case with the higher pressure that confirms the observation. For the lower value of pressure (e.g. 4×10^5 Pa) the collisions were distributed rather uniformly over the whole length.

This information yields the first indication that enables the prediction of stress and strain in the construction and/or possible fracture points.

5.3. The influence of particle diameter

Particle diameter is another parameter of interest. Bigger particles usually tend to accelerate slower due to their higher inertia. On the contrary, they also have a higher mass which is of importance when collisions with an obstacle are considered. Another important issue is that they do not intensively interact to sudden changes in the flow direction or magnitude (like eddies) so that the shape of the flowing cloud is also different.

Fig. 8 shows particle snapshots for two cases, where the particle diameter was equal to 4 and 6 mm. For both cases, the time was 60 ms; hence, these figures correspond to Fig. 2b. We can observe that the "heavier" particles also have a higher inertia and they are less subject to sudden changes of the flow.

The momentum distribution of particles that collided with the beam during the period 800 ms was also analysed. The results are shown in Fig. 9. In all the cases, the initial pressure was the same and equal to 8×10^5 Pa. Particle diameter was the parameter that varied at 2, 3, 4 and 6 mm.

This time the results were more difficult to predict and less obvious conclusions were arrived at. For the smallest particles (2 mm) the focus on the higher part of the beam was observed (note that the same curve is also shown in Fig. 7). As the particles became bigger (3 mm), formation of more uniform distribution was observed as the particles tended to fall due to gravity and their initial velocity was lower. An interesting observation was made for particles of diameter 4 mm that tended to collide only with the lower part of the obstacle, while particles of diameter 6 mm hardly touched the obstacle.

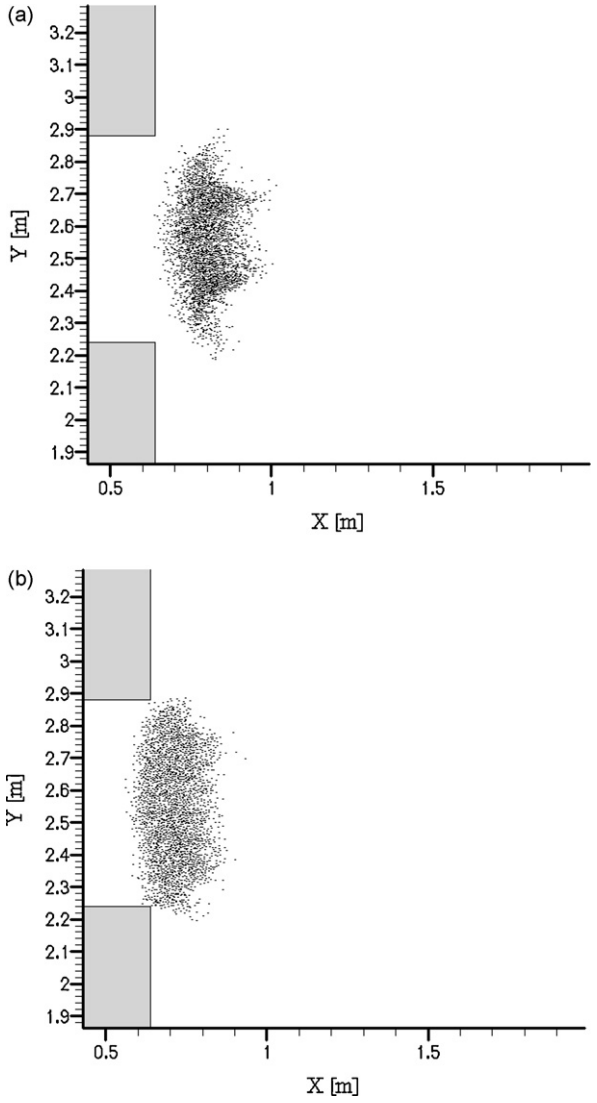

Fig. 8. Snapshots of particle position for two values of particle diameter: (a) 4 mm and (b) 6 mm.

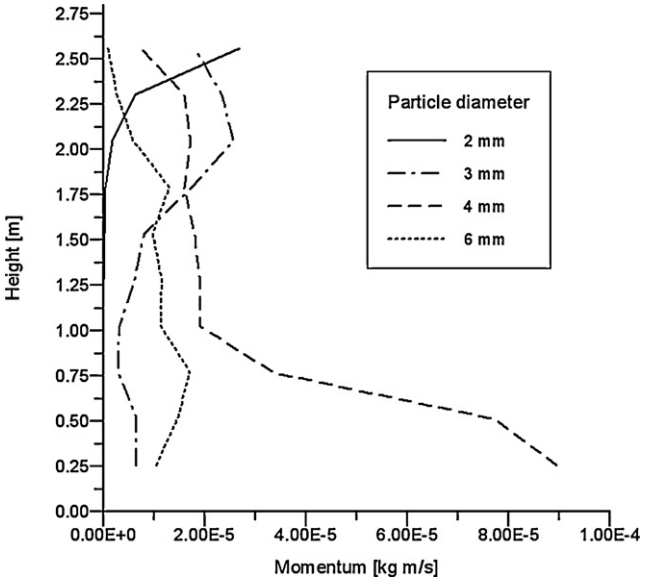

Fig. 9. The distribution of the momentum of particles that have collided with the obstacle for various values of the particle diameter.

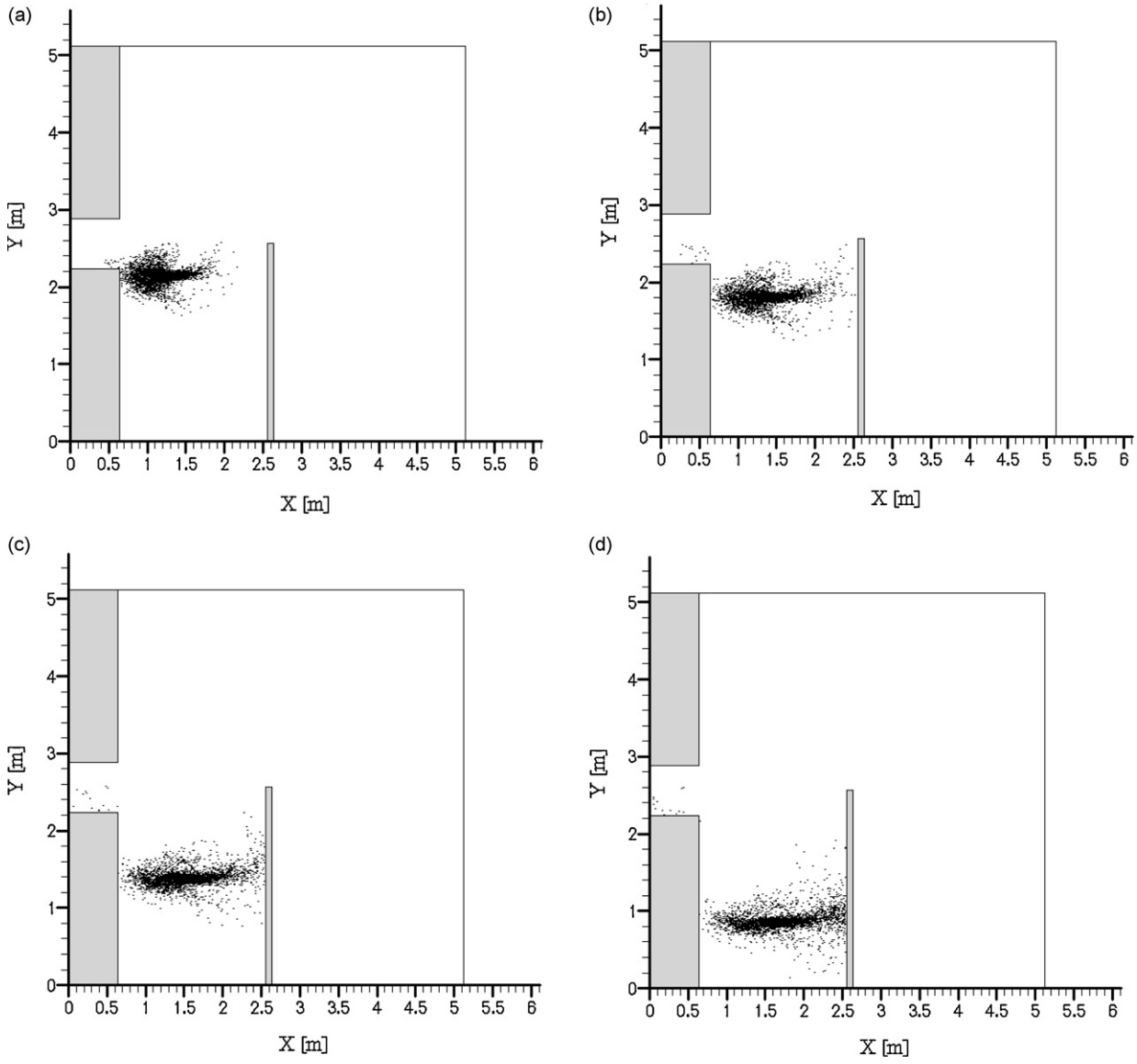

Fig. 10. Snapshots of particle positions for various points in time: (a) 300 ms, (b) 400 ms, (c) 500 ms, and (d) 600 ms. The initial pressure in the high-pressure section was 8×10^5 Pa and particle diameter was 6 mm.

This is also illustrated in Fig. 10, as snapshots of particle position for different points in time: 300, 400, 500 and 600 ms and for the case where the particle diameter was 6 mm. This figure can be directly compared to Fig. 6, where the particle diameter was smaller: gravity force and higher inertia of the heavier particles play a role here.

In this section the influence of particle diameter has been analysed. The increase of diameter also leads to increase in particle concentration, i.e. particle mass per unit volume.

5.4. The influence of number of particles

A comparison of the following two cases is of interest. Debris concentration (or the total mass) is the same for both cases, but the number of particles is different. This also leads to the conclusion that the particle diameter must change if the mass is to be kept a constant, i.e. the following relation can be easily derived (still assuming the spherical shape of the particles):

$$d_1 = d_2 \sqrt[3]{\frac{N_2}{N_1}} \tag{11}$$

where d is particle diameter and N is the total number of particles in the cloud, while 1 and 2 denote two different cases that are being analysed.

The two simulations are compared. The first has already been discussed above: particle diameter was equal to 2 mm, the initial pressure in the chamber was 8×10^5 Pa and the total number of particles was 2560. In the second simulation, the total number of particles was four times smaller, i.e. 640. To have the same mass of debris, the particle diameter had to be higher and equal to 3.1748 mm (see the above mentioned relation).

The results are shown in Fig. 11 and illustrate the influence. However, it appears that even though the debris mass is the same, the number of particles will have a crucial effect.

This can be supported by theoretical analysis that does not require use of any simulating techniques as above. Let us assume that particles are subject to a one-dimensional gas flow that is not influenced by the particles and that the relative Reynolds number is high (Newton's law is valid, i.e. drag force coefficient is constant). Also gravity does not act in this direction. The total momentum of the particle cloud is defined as: $M = N \cdot u_p \cdot m$, where N is the total number of particles in the cloud, u_p is their velocity (assum-

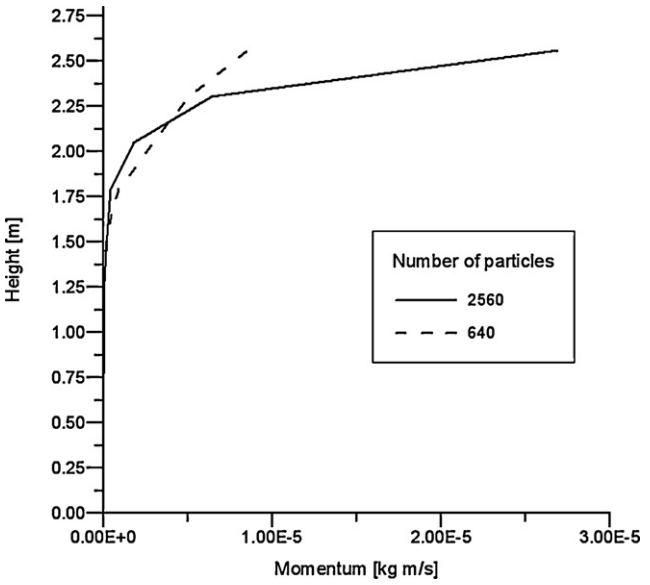

Fig. 11. The distribution of the momentum of particles that have collided with the obstacle for two different total number of particles: 2560 and 640.

ing now that it is the same for all the particles) and m is mass of each particle.

By repeating Eq. (2) we obtain (we multiply both sides by N and assume that all the particles have the same mass and velocity):

$$N \cdot m \cdot \frac{du_p}{dt} = N \cdot f \tag{12}$$

which is the same as:

$$\frac{dM}{dt} = N \cdot f \tag{13}$$

with M being defined above.

Combining Eq. (13) and Eq. (3) yields:

$$\frac{dM}{dt} = N \cdot C_D \frac{\pi d^2}{8} \rho (u_g - u_p)^2 \tag{14}$$

where we additionally specify the projected area A_p as $\pi d^2/4$, as well as: $(u_g - u_p)\left|u_g - u_p\right| \equiv (u_g - u_p)^2$ since we assume that the flow is only in one direction.

This can be further modified to:

$$\frac{dM}{dt} = N \cdot C_D \frac{\pi d^2}{8} \rho (m \cdot N \cdot u_g - m \cdot N \cdot u_p)^2 \frac{1}{(m \cdot N)^2} \tag{15}$$

that yields:

$$\frac{dM}{dt} = \frac{C_D}{N} \frac{4.5}{\rho_p^2 \cdot \pi \cdot d^4} \rho \left(N \cdot u_g \cdot \rho_p \frac{\pi d^3}{6} - M \right)^2 \tag{16}$$

since particle mass is: $m = \rho_p \cdot \pi \cdot d^3/6$

By solving this differential equation, the momentum of the particle cloud for any point in time can be found with the above mentioned assumptions (the initial momentum of the particles is zero):

$$M = N \cdot d^3 \left(u_g \cdot \rho_p \cdot \pi/6 - \frac{1}{(4.5 C_D \rho/\rho_p^2 \cdot \pi \cdot d)t + (6/u_g \cdot \rho_p \cdot \pi)} \right) \tag{17}$$

As we analyse the two cases, where the total mass of the particles is the same and what differs is the total number of particles and their diameter, Eq. (17) can be written for these two situations, i.e. $M_1 = f(d_1, N_1)$ and $M_2 = f(d_2, N_2)$ for a given point in time t. For instance for the first case:

$$M_1 = N_1 \cdot d_1^3 \left(u_g \cdot \rho_p \cdot \pi/6 - \frac{1}{(4.5 C_D \rho/\rho_p^2 \cdot \pi \cdot d_1)t + (6/u_g \cdot \rho_p \cdot \pi)} \right) \tag{18}$$

And in the same manner one can write a similar formula for the second case (subscript 1 has to be replaced with 2):

$$M_2 = N_2 \cdot d_2^3 \left(u_g \cdot \rho_p \cdot \pi/6 - \frac{1}{(4.5 C_D \rho/\rho_p^2 \cdot \pi \cdot d_2)t + (6/u_g \cdot \rho_p \cdot \pi)} \right) \tag{19}$$

Taking into account the relation defined in Eq. (11), the total momentum for the first case (Eq. (18)) can be changed to the following relation:

$$M_1 = N_2 \cdot d_2^3 \left(u_g \cdot \rho_p \cdot \pi/6 - \frac{1}{(4.5 C_D \rho/\rho_p^2 \cdot \pi \cdot d_2)\sqrt[3]{N_1/N_2}\, t + (6/u_g \cdot \rho_p \cdot \pi)} \right) \tag{20}$$

Thus: if $N_1 > N_2$, the total momentum for the first case (Eq. (20)) is higher than for the second case (Eq. (19)). This explains the results shown in Fig. 11.

Nevertheless, it must be noted that this discussion does not take into account some more complex phenomena, though it explains the fundamental behaviour of the debris cloud.

5.5. The influence of obstacle location

As expected, the position of the beam is one of the most important parameters. As the obstacle is located closer to the chamber exit, the particles may collide with a higher momentum. However, the closer location may also lead to some unexpected phenomena due to the fact that any additional elements in the domain will strongly influence the gas flow, which may later alter the motion of the debris.

As earlier, the total momentum of the particles that collide with the obstacle during period of 800 ms was analysed. The results are shown in Fig. 12 as three curves corresponding to the various locations of the obstacle.

This time the results may not appear obvious: for the situation where the beam is located at the distance 256 computational cells, the total momentum is observed to be actually higher in comparison to the case where the beam is placed much closer to the explosion zone. The explanation of this surprising observation is as follows: the beam also hinders the gas flow, which is suddenly turned. This is especially visible for the case when the obstacle is situated closer to the chamber exit. Another important issue is the lower "volume" of the space between the obstacle and the left side of the domain. The first pressure wave moves down and then returns as a reflected wave, and this phenomenon is stronger for a "narrower" domain. This leads to the well known, though surprising observation that the particles do not interact with the beam as intensively as it is located at a further distance.

Fig. 13 illustrates this situation: a snapshot of particle position is shown as they approach the obstacle. The figure also shows the vectors of the particle velocities and a clear motion upwards may be observed. In order to better illustrate this process, we show also the gas pressure distribution for the same point in time (see Fig. 14).

However, this observation cannot be expected for the case where the particles have a higher inertia. Therefore, results for bigger particles, namely of diameter 4 mm (see Fig. 15) are shown.

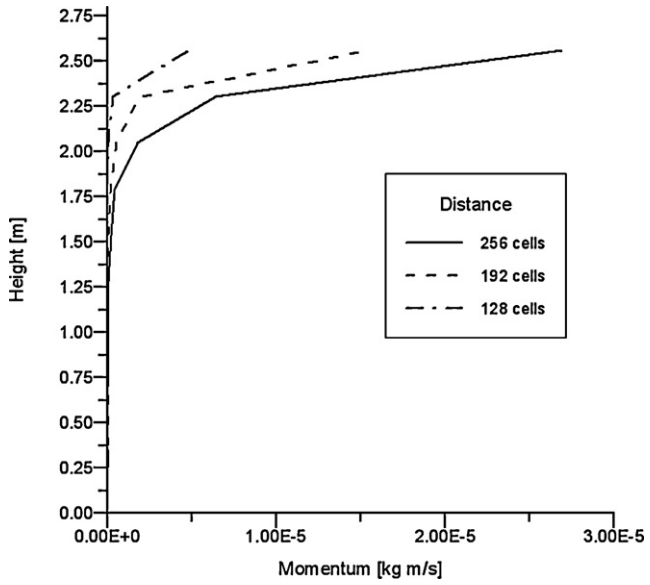

Fig. 12. The distribution of the momentum of particles that have collided with the obstacle for various locations of the beam. Particle diameter was 2 mm.

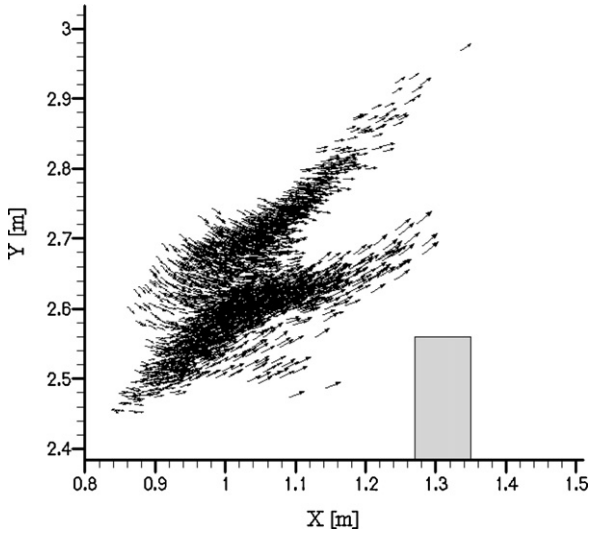

Fig. 13. Particle cloud motion after 50 ms. The beam was located at distance 128 cells and the particle diameter was 2 mm.

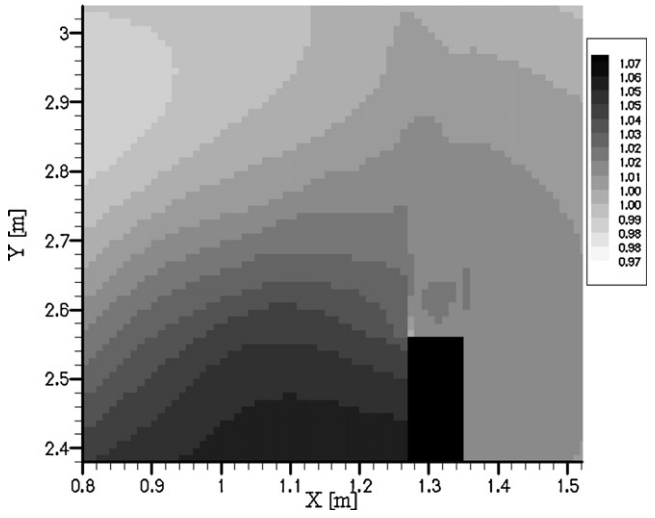

Fig. 14. Gas pressure distribution after 50 ms. The beam was located at distance 128 cells and the particle diameter was 2 mm.

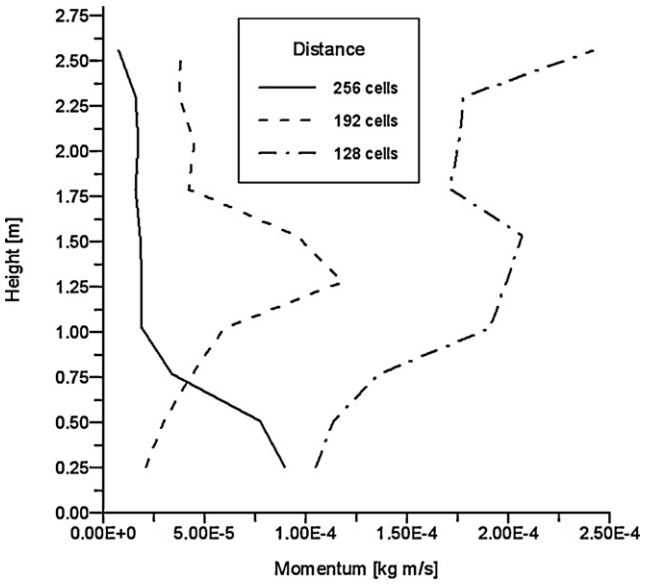

Fig. 15. The distribution of the momentum of particles that have collided with the obstacle for various locations of the beam. Particle diameter was 4 mm.

This time there is a clear trend that corresponds to our expectations: as the distance increases, the particles collide with a lower momentum.

The main conclusion drawn here is that two opposite mechanisms exist: strength of the explosion and particle inertia. If the former dominates, results are obtained that appear to be more obvious: this usually describes stronger explosions. For weaker explosions (lower pressure or smaller domain), the behaviour of the debris becomes dependent on geometry.

6. Concluding remarks

In this research we showed that the Lagrangian approach for solid particle modelling can be used to simulate the flow of debris. The gas flow was based on the standard Navier–Stokes equations where the influence of the particles was implemented as the source terms. The algorithm accounts for collisions, especially with obstacles. The chemical reactions were ignored, as the objective was only to analyse the consequences of explosions and not their exact course.

Other assumptions were also made. All the particles were assumed to be spherical and of the same size. The former made it possible to use quite accurate and well-tested models, while the latter can be easily modified by assuming any particle size distribution. In this paper we did not wish to focus on it: the objective was rather not to simulate a real case, but to investigate the influence of various parameters like particle size and mass, the initial pressure and the location of the obstacle

In future studies we are, however, planning to influence a more real case as well. It will be assumed that the particle size can vary in the debris cloud and the size distribution is specified. This will influence both the behaviour of the cloud since smaller particles do not behave in the same way as the bigger ones, as well as the gas motion.

The parameters (particle size, pressure and the obstacle location) were tested for some arbitrary geometry and initial data. We must emphasize that the mathematical model is able to also cope with other cases, but we did not focus on them. Analysis of the results led to interesting observations and revealed complex phenomena, where perhaps the most important was the coupling between the fluid flow and the debris behaviour.

The ultimate goal would be to implement models describing the behaviour of the solid structure and the debris. This is outside the scope of this research, as the main focus was an analysis of the mechanisms leading to a possible debris–obstacle interaction, not the consequences.

Acknowledgments

The author is grateful to the colleagues from The University of Bergen for helpful discussions, especially regarding the modelling and interpretation of results.

References

[1] C. Crowe, M. Sommerfeld, Y. Tsuji, Multiphase Flows with Droplets and Particles, CRC Press LLC, 1998.
[2] R.K. Eckhoff, Explosion Hazards in the Process Industries, Gulf Professional Publishing, 2005.
[3] R.K. Eckhoff, Dust Explosions in the Process Industries, Gulf Professional Publishing, 2003.
[4] J.K. Clutter, J.T. Mathis, M.W. Stahl, Modelling environmental effects in the simulation of explosion events, Int. J. Impact Eng. 34 (2007) 973–989.
[5] Y. Lu, K. Xu, Prediction of debris launch velocity of vented concrete structures under internal blast, Int. J. Impact Eng. 34 (2007) 1753–1767.
[6] B.M. Luccioni, R.D. Ambrosini, R.F. Danesi, Analysis of building collapse under blast loads, Eng. Struct. 26 (2004) 63–71.
[7] Y. Shi, H. Hao, Z.X. Li, Numerical derivation of pressure-impulse diagrams for prediction of RC columns damage to blast loads, Int. J. Impact Eng. 35 (2008) 1213–1227.
[8] G.K. Schleyer, M.J. Lowak, M.A. Polcyn, G.S. Langdon, Experimental investigation of blast wall panels under shock pressure loading, Int. J. Impact Eng. 34 (2007) 1095–1118.
[9] M.A. Sprague, T.L. Geers, A spectral-element/finite-element analysis of a ship-like structure subjected to an underwater explosion, Comput. Methods Appl. Mech. Eng. 195 (2006) 2149–2167.
[10] M.R. Ross, C.A. Felippa, K.C. Park, M.A. Sprague, Treatment of acoustic fluid–structure interaction by localized Lagrange multipliers: formulation, Comput. Methods Appl. Mech. Eng. 197 (2008) 3057–3079.
[11] O. Igra, J. Jiang, Head on collision of a planar shock wave with a dusty gas layer, Shock Waves 18 (2008) 411–418.
[12] I.A. Bedarev, Y.A. Gosteev, A.V. Fedorov, Shock-wave-initiated lifting of particles from a cavity, J. Appl. Mech. Tech. Phys. 48 (2007) 17–26.
[13] A.V. Federov, I.A. Fedorchenko, I.V. Leont'ev, Mathematical modeling of two problems of wave dynamics in heterogeneous media, Shock Waves 15 (2006) 453–460.
[14] T. Suzuki, Y. Sakamura, O. Igra, T. Adachi, S. Kobayashi, A. Kotani, Y. Funawatashi, Shock tube study of particles' motion behind a planar shock wave, Meas. Sci. Technol. 16 (2005) 2431–2436.
[15] O. Igra, G. Hu, J. Falcovitz, B.Y. Wang, Shock wave reflection from a wedge in a dusty gas, Int. J. Multiphase Flow 30 (2004) 1139–1169.
[16] O. Igra, X. Wu, G.Q. Hu, J. Falcovitz, Shock wave propagation into a dust-gas suspension inside a double-bend conduit, Shock wave propagation into a dust-gas suspension inside a double-bend conduit, J. Fluids Eng.-T. ASME 124 (2002) 483–491.
[17] N. Thevand, E. Daniel, Numerical study of the lift force influence on two-phase shock tube boundary layer characteristics, Shock Waves 11 (2002) 279–288.
[18] T. Saito, Numerical analysis of dusty-gas flows, J. Comput. Phys. 176 (2002) 129–144.
[19] R. Klemens, P. Kosinski, P. Wolanski, V.P. Korobeinikov, V.V. Markov, I.S. Menshov, I.V. Semenov, Numerical study of dust lifting in a channel with vertical obstacles, J. Loss Prevent. Proc. 14 (2001) 469–473.
[20] B. Khasainov, A. Kuhl, S. Victorov, P. Neuwald, Model of non-premixed combustion of aluminium–air mixtures, in: Proceedings of the 14th APS Topical Conference on Shock Compression of Condensed Matter, Baltimore, MD, 2005.
[21] E.F. Toro, Riemann Solvers and Numerical Methods for Fluid Dynamics, Springer–Verlag, Berlin, 1999.
[22] P. Kosinski, On shock wave propagation in a branched channel with particles, Shock Waves 15 (2006) 13–20.
[23] P. Kosinski, Numerical investigation of explosion suppression by inert particles in straight ducts, J. Hazard. Mater. 154 (2008) 981–991.
[24] V.M. Boiko, V.P. Kiselev, S.P. Kiselev, A.N. Papyrin, S.V. Poplavsky, V.M. Fomin, Shock wave interaction with a cloud of particles, Shock Waves 7 (1997) 275–285.